Saimaa University of Applied Sciences
Faculty of Technology, Lappeenranta
Degree Programme in Mechanical Engineering and Production Technology

David Bolek

Simplification methods for reducing computational effort in mechanical analysis

Thesis 2018

Abstract

David Bolek
Simplification methods for reducing computational effort in mechanical analysis, 44 pages
Saimaa University of Applied Sciences
Faculty of Technology, Lappeenranta
Degree Programme in Mechanical Engineering and Production Technology

Thesis 2018
Instructor: D.Sc. (Tech.) Janne Heikkinen, Lappeenranta University of Technology

Many finite element models have large amount of degrees of freedom, analysing such models can take tens of hours. The main goal of the bachelor thesis was to present model simplification methods which can help to reduce solution time.

The thesis consists of two parts. The first part of this work describes four simplification methods and their use in practice. In the second part, the applicability of each method is demonstrated on several examples. The functionality of simplification methods is verified comparing the full model analysis and the simplified model analysis. The thesis focuses mainly on static and modal analysis. The analyses are performed using software ANSYS Workbench 18.0 and MATLAB.

Keywords: model simplification methods, Guyan reduction, symmetry, geometry simplification, multibody system, static analysis, modal analysis, ANSYS, MATLAB

Table of contents

Terminology

Term	Definition	Unit
$\propto$	Sector angle	$[rad]$
B	Breadth of the cross-section of the beam	$[m]$
C_1, C_2	Amplitudes of the angular displacements	$[rad]$
d	Nodal diameter	$[-]$
d_1, d_2	Diameters of the shafts	$[m]$
D_1, D_2	Diameters of the disks	$[m]$
δ	Relative error	$[\%]$
$\Delta l_1, \Delta l_2$	Angular displacements	$[rad]$
E, G	Young's modulus and shear modulus	$[Pa]$
f_0	Natural frequency	$[s^{-1}]$
f_1, f_2	Natural frequencies of the disks	$[s^{-1}]$
f_S, f_F	Natural frequencies of the simplified and full model	$[s^{-1}]$
F_m, F_s	External forces acting on the master and slave degrees of freedom	$[N]$
φ	Initial phase angle	$[rad]$
φ_1, φ_2	Angular displacements of the disks	$[rad]$
H	Height of the cross-section of the beam	$[m]$
I	Moment of inertia	$[kg \cdot m^2]$
I_1, I_2	Moments of inertia of the disks	$[kg \cdot m^2]$
J_{P_1}, J_{P_2}	Polar moments of inertia of the shafts	$[mm^4]$
k	Harmonic index	$[-]$
k	Stiffness	$[Nm]$
$k_{11}, k_{12}, k_{21}, k_{22}$	Elements of the stiffness matrix	$\left[\frac{Nm}{rad}\right]$
k_{T_1}, k_{T_2}	Torsional stiffnesses of the springs	$\left[\frac{Nm}{rad}\right]$
K	Stiffness matrix of the system	$[N \cdot m^{-1}]$
K_G	Reduced stiffness matrix of the system	$[N \cdot m^{-1}]$
$K_{mm}, K_{ms}, K_{sm}, K_{ss}$	Master and slave elements of the stiffness matrix	$[N \cdot m^{-1}]$
L	Equivalent length	$[m]$
L_1, L_2	Lengths of the shafts	$[m]$
λ_1, λ_2	Eigenvalues	$[s^{-2}]$

Term	Definition	Unit
m	Integer	$[-]$
m	Mass of a body	$[kg]$
m_1, m_2	Masses of the disks	$[kg]$
M	Mass matrix of the system	$[kg]$
M_G	Reduced mass matrix of the system	$[kg]$
$M_{mm}, M_{ms}, M_{sm}, M_{ss}$	Master and slave elements of the mass matrix	$[kg]$
n	Number of the sectors	$[-]$
ν	Eigenvector	$[-]$
Ω_0	Angular natural frequency	$[s^{-1}]$
Ω_1, Ω_2	Angular natural frequencies of the disks	$[s^{-1}]$
π	Mathematical constant	$[-]$
ρ	Density	$[kg \cdot m^{-3}]$
t	Time	$[s]$
T_1, T_2	Thicknesses of the disks	$[m]$
T_{D1}, T_{D2}	Reaction torques	$[Nm]$
T_G	Coordinate transformation or global mapping matrix	$[-]$
U^A_{High}, U^A_{Low}	Vector of displacement and rotational degrees of freedom of the basic sector's high and low edge	$[-]$
U^B_{High}, U^B_{Low}	Vector of displacement and rotational degrees of freedom of the duplicate sector's high and low edge	$[-]$
x_m, x_s	Displacements of the master and slave degrees of freedom	$[m]$

Abbreviation	Definition
3D	Three-dimensional
CAD	Computer aided design
DOF	Degrees of freedom
FE	Finite element
FEA	Finite element analysis
FEM	Finite element method
RPM	Revolutions per minute

1 Introduction

An integral part of the product's design is performing simulations, which can model a stress, deformations or dynamical behaviors of the product. One of the most commonly used simulations is based on Finite element method FEM also called Finite element analysis FEA. The basic principle of this method is dividing a model into small pieces called finite elements. Each finite element is described with a set of equations. Those equations are then assembled into larger set of equations describing the whole model [1]. Static analysis of the simple model consisting of a small number of finite elements can be quickly calculated on the paper, however with more complicated models a number of finite elements and thus, a number of equations increases. In that case, computers are involved.

Nowadays, models are larger and more complex and even using computers with higher performance, calculations can last tens of hours. Right from the beginning of the FEM analysis, engineers had to deal with limited computation resources. Later, companies started to demand shorter time for the development of the products. Therefore, a need of methods dealing with large complex mechanical systems arose. The main question was how the model can be simplified so that it will use less computational effort and simultaneously results would be precise enough compared with a full model analysis results.

The aim of the thesis is to present four widely used model simplification methods which can reduce computation effort in mechanical analysis. These methods are Guyan static reduction method, Symmetry, Geometry simplification method and Multibody system.

The thesis is divided into two parts. In the first part, simplification methods are described along with their advantages, disadvantages and usage. The second part demonstrates the functionality of methods on simple and understandable examples.

2 Model simplification methods

During the last decades many simplification methods for reducing the computation time have been developed. In this chapter, four methods are presented. These methods are Guyan static reduction method, Symmetry, Geometry simplification method and Multibody system. Each method has its own advantages and disadvantages, and can be used in various cases.

2.1 Guyan static reduction method

As mentioned in the Introduction, large models can have several millions degrees of freedom and analysing such models would take lots of time. The idea of Guyan reduction method is that when a structure is excited some degrees of freedom may have a more significant response than the others. By eliminating those degrees of freedom, which do not contribute on the model's response, we can significantly reduce the model. [1]

2.1.1 Definition

All degrees of freedom in the discrete model can be re-ordered as master degrees of freedom (retained) and slave degrees of freedom (discarded) so that the system equation of motion can be written as

$$\begin{bmatrix} M_{mm} & M_{ms} \\ M_{sm} & M_{ss} \end{bmatrix} \begin{Bmatrix} \ddot{x_m} \\ \ddot{x_s} \end{Bmatrix} + \begin{bmatrix} K_{mm} & K_{ms} \\ K_{sm} & K_{ss} \end{bmatrix} \begin{Bmatrix} x_m \\ x_s \end{Bmatrix} = \begin{Bmatrix} F_m \\ F_s \end{Bmatrix} \tag{1}$$

where *m* refers to master degrees of freedom and *s* indicates slave degrees of freedom.

The Guyan approximation considers static solution in which neglects the inertia effects [2] so that Eq. (1) condense to

$$\begin{bmatrix} K_{mm} & K_{ms} \\ K_{sm} & K_{ss} \end{bmatrix} \begin{Bmatrix} x_m \\ x_s \end{Bmatrix} = \begin{Bmatrix} F_m \\ F_s \end{Bmatrix} \tag{2}$$

After multiplication of matrices Eq. (2) is in the form

$$K_{mm}x_m + K_{ms}x_s = F_m \tag{3}$$

$$K_{sm}x_m + K_{ss}x_s = F_s \tag{4}$$

Guyan (1965) assumed that external forces acting on the slave degrees of freedom are equal to zero, $F_s = 0$, hence Eq. (4) leads to

$$K_{sm}x_m + K_{ss}x_s = F_s \tag{5}$$

and after separation the x_s, it is received

$$x_s = -{K_{ss}}^{-1}K_{sm}x_m \tag{6}$$

Eq. (6) shows relations between master and slave displacements. Displacement vector from the Eq. (6) can be written as

$$x = \begin{Bmatrix} x_m \\ x_s \end{Bmatrix} = T_G x_m \tag{7}$$

where T_G is *coordinate transformation* matrix or *global mapping matrix*

$$T_G = \begin{bmatrix} I \\ -{K_{ss}}^{-1}K_{sm} \end{bmatrix} \tag{8}$$

Then reduced stiffness matrix is

$$K_G = T_G^T K T_G \tag{9}$$

$$K_G = K_{mm} - K_{ms}K_{ss}^{-1}K_{sm} \tag{10}$$

And reduced mass matrix [3] is

$$M_G = T_G^T M T_G \tag{11}$$

$$M_G = M_{mm} - K_{sm}^T K_{ss}^{-1} M_{sm} - M_{ms}K_{ss}^{-1}K_{sm} + K_{sm}^T K_{ss}^{-1} M_{mm} K_{ss}^{-1} K_{sm} \tag{12}$$

Substituting Eq. (7) to the Eg. (1) and multiplying this expression by T_G results in a reduced-order system [1]

$$T_G^T M T_G \ddot{x_m} + T_G^T K T_G x_m = T_G^T F \tag{13}$$

2.1.2 Numerical demonstration

Creating of the reduced mass and stiffness matrices is presented on the following example. In Figure 1 3 DOF mass-stiffness system is shown. A mass $m = 1\ kg$ and a stiffness $k = 1\ N \cdot m^{-1}$. The stiffness and mass matrices of the system can be quickly obtained as

$$K = \begin{bmatrix} 2 & -1 & 0 \\ -1 & 2 & -1 \\ 0 & -1 & 1 \end{bmatrix}, \qquad M = \begin{bmatrix} 1 & 0 & 0 \\ 0 & 1 & 0 \\ 0 & 0 & 1 \end{bmatrix}$$

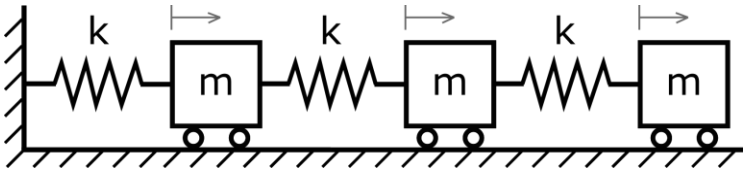

Figure 1. 3 DOF mass-stiffness system

Assuming the first and the third degree of freedom are selected as master degrees of freedom, rows and columns in the stiffness and mass matrices can be reordered as

$$\begin{bmatrix} K_{mm} & K_{ms} \\ K_{sm} & K_{ss} \end{bmatrix}, \qquad \begin{bmatrix} M_{mm} & M_{ms} \\ M_{sm} & M_{ss} \end{bmatrix}$$

In our case, the mass matrix remains the same and for the reordering of the stiffness matrix two steps can be done. Firstly, the 2nd row will change place with the 3rd row, and secondly, the 2nd column will change a place with the 3rd column as shown below

$$\begin{bmatrix} 2 & -1 & 0 \\ -1 & 2 & -1 \\ 0 & -1 & 1 \end{bmatrix} \rightarrow \begin{bmatrix} 2 & -1 & 0 \\ 0 & -1 & 1 \\ -1 & 2 & -1 \end{bmatrix} \rightarrow \begin{bmatrix} 2 & 0 & -1 \\ 0 & 1 & -1 \\ -1 & -1 & 2 \end{bmatrix}$$

From this can be extracted

$$K_{mm} = \begin{bmatrix} 2 & 0 \\ 0 & 1 \end{bmatrix}, \; K_{ss} = [2], \; K_{ms} = \begin{bmatrix} -1 \\ -1 \end{bmatrix}, \; K_{sm} = [-1 \quad -1]$$

Then a reduced stiffness matrix is calculated according to the Eq. (10)

$$K_G = K_{mm} - K_{ms}K_{ss}^{-1}K_{sm} = \left\{ \begin{bmatrix} 2 & 0 \\ 0 & 1 \end{bmatrix} - \begin{bmatrix} -1 \\ -1 \end{bmatrix} [2]^{-1} [-1 \quad -1] \right\} = \begin{bmatrix} 1.5 & -0.5 \\ -0.5 & 0.5 \end{bmatrix}$$

In the same way a reduced mass matrix can be calculated using Eq. (12).

2.1.3 How to select master coordinates

The question is how the master degrees of freedom should be selected. Guyan approximation neglects inertias associated with slave degrees of freedom, therefore master degrees of freedom are chosen where the inertia, damping and load is high. [4]

2.1.4 Advantages and disadvantages

The main advantages of Guyan reduction method are that it is computationally efficient and easy to implement. The method is also used in many commercial FEA softwares including MSC-NASTRAN and ANSYS [5].

The main disadvantage of Guyan reduction method is that it neglects inertias associated with the slave degrees of freedom. The method is unacceptable for systems with high mass/stiffness ratios. The method is exact for static problems, but for dynamic problems the accuracy is very low and depends on selection of masters. Furthermore, with increasing natural frequencies, the error is increasing as well, therefore this method is suitable only for calculating lower modes. [3], [5]

2.2 Symmetry

Many objects and structures have some kind of symmetry. Using the symmetry, the system's total number of degrees of freedom can be significantly reduced, and therefore solution time to solve the problem. The use of symmetry does not cause the loss of accuracy. Furthermore, a designer does not have to create full model, but just its symmetrical part. [3], [6]

The symmetry can be used if the physical system exhibits symmetry in geometry, loads, constraints and material properties. [7]

Types of symmetry (Figure 2)

- Axial symmetry
- Cyclic or rotational symmetry
- Planar or reflective symmetry
- Repetitive or translational symmetry [7]

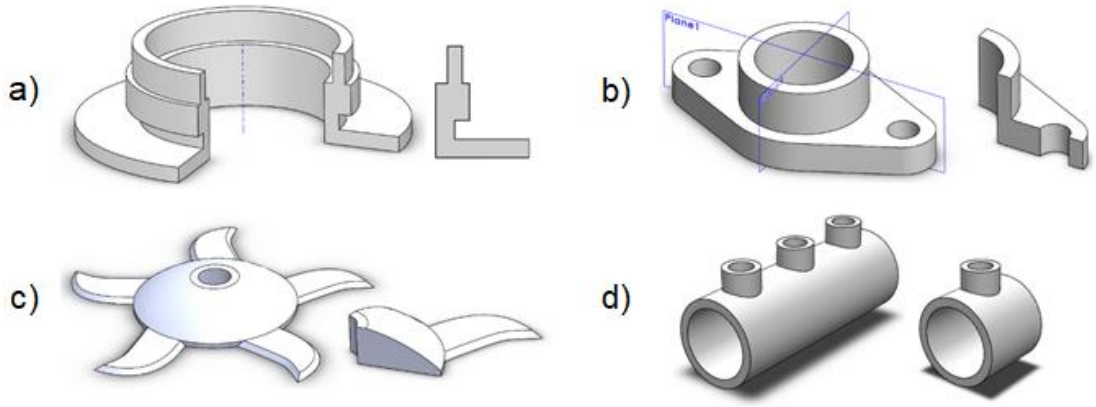

Figure 2. Types of symmetry: a) axial, b) reflective/planar, c) cyclic/rotational and d) repetitive/translational

2.2.1 Axial symmetry

The structure has an axial symmetry if it can be generated by rotating a planar shape about an axis, e.g. plates, vases, cones and pressure vessels [7].

2.2.2 Planar or reflective symmetry

The most common type of symmetry is planar or reflective symmetry. In this case, model has one or more planes of symmetry [3].

The beam presented in Figure 3 is symmetric and also loading applied on the beam is symmetrical, therefore it is enough to take only half of the beam using the symmetric boundary conditions to perform analysis. Symmetric boundary conditions are zero displacement in the normal direction to the plane of symmetry and no rotation by the plane of symmetry.

In case that the structure is symmetric but the loading is anti-symmetric, a so called anti-symmetric problem occurs [8]. Considering the presented beam in Figure 3, the problem becomes anti-symmetric if one of the forces is acting in the opposite direction. Then the anti-symmetric boundary conditions are zero displacements in normal and parallel direction to the plane of symmetry and free rotation by the plane of symmetry.

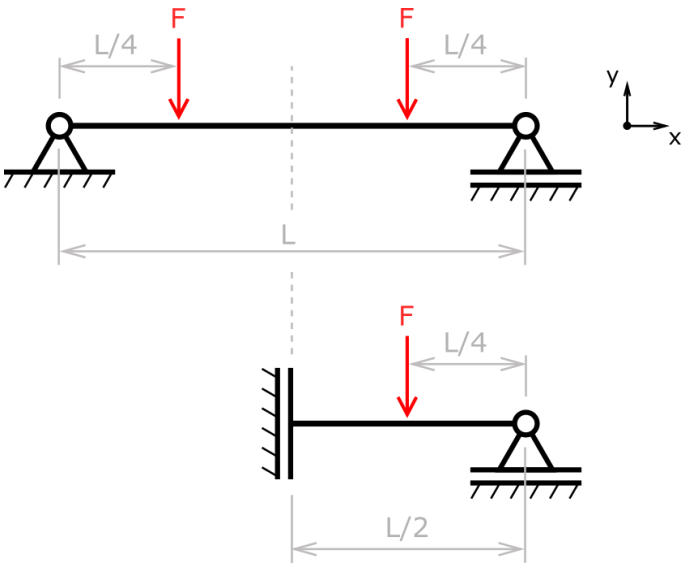

Figure 3. Symmetric beam

2.2.3 Repetitive or translational symmetry

Repetitive or translation symmetry prevails in structures where several sections are repeated, e.g. long pipes with evenly spaced cooling fins [7]. Only one section can be modelled to perform analysis.

2.2.4 Cyclic or rotational symmetry

Cyclic or rotation symmetry is the geometrical repetition of sections about a central axis [7]. An example is a turbine.

2.3 Simplification of the geometry

The CAD model may be very detailed, containing a large number of faces and edges and some of them are often smaller than the element size. This can lead to very complex meshing with poorly-shaped elements or over-densified elements. Such mesh not only increases time for the analysis but also produces not accurate results. In this case, it is convenient to simplify a model and thus, to create a proper mesh and also to decrease the number of degrees of freedom. Another reason for simplifying the model is that you can compare a model with theory which is mostly based on simple models. [8], [9]

There are many simplification techniques [10], e.g. face clustering [11], edge decimation based approach [12], decimation-cell transformation based technique [13] and others. One of the most used techniques is removing details and features such as chamfers, fillets, rounds and holes. The critical part is to determine whether those features are important or not important for further analysis, in other words, how much the model can be simplified to still obtain accurate results [14].

An example of a model with features, which can be removed or which cannot, is illustrated in Figure 4. Considering modal analysis, this sheet metal model contains several holes, projections and fillets which are very small and do not contribute to its lowest mode shapes. Those features can be removed and then, the simplified model is obtained including all necessary features which can affect the analysis.

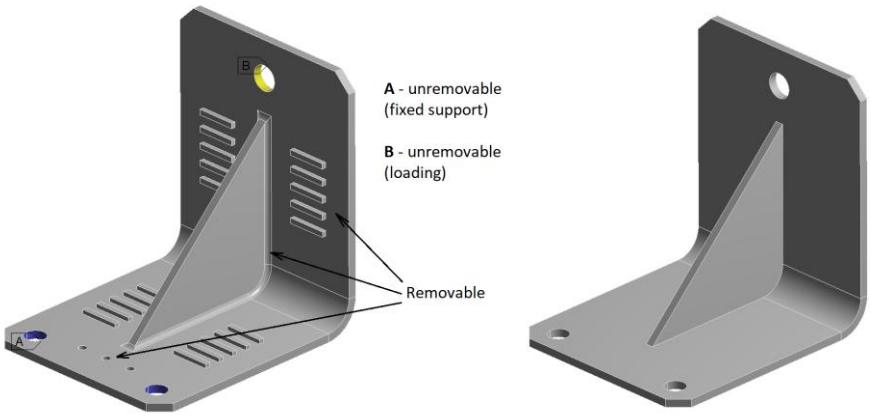

Figure 4. Left – full model, right – simplified model

Considering a complex model, trying to manually simplify such a model can be very time-consuming. Therefore, many algorithms were created, which can extract CAD model information, remove unnecessary details and thus, make the simplification process automatic.

2.4 Multibody system

The number of natural frequencies of the finite element model corresponds to its number of degrees of freedom. The complex structures might have hundreds of

thousands of degrees of freedom and thus, the same amount of natural frequencies, however only ten or twenty modes could be enough to capture the overall dynamic behavior of the structure [15].

The main goal of a multi-body model simplification is to create such a model which can describe real systems behaviors using only the minimum of model entities and ignoring the other features. This leads to dramatic reduction of the number of degrees of freedom. Basically, the problem is to know which features should be neglected and which should sustain in a particular situation [16].

For example, a grinder mounted on the pedestal can be simplified as a vertical beam vibrating in horizontal direction, with a mass at the top, shown in Figure 5. It makes the grinder to be only 1 DOF system. Considering that the beam is fixed to the floor, the bending stiffness of the beam can be calculated as [17]

$$k = \frac{3EI}{L^3} \tag{14}$$

where E is Youngus Modulus, I is a moment of inertia of the beam and L is the equivalent length of the beam.

Then the natural frequency of the beam is [17]

$$f_0 = \frac{1}{2\pi}\sqrt{\frac{k}{m}} \tag{15}$$

where k is the beam stiffness and m is a mass of the grinder.

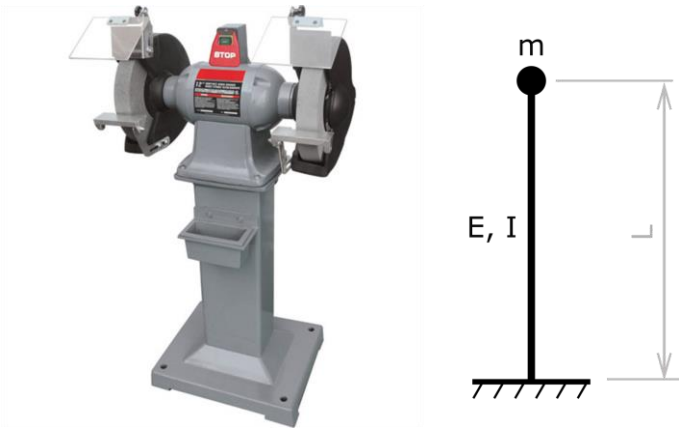

Figure 5. Grinder on the pedestal on the left, 1 DOF model on the right (modified figure [18])

Although this example may seem to be simple and easy to implement, creating a simplified system many times requires knowledge based on experience.

2.5 Summary

In the previous chapters, simplification methods were introduced. Table 1 summarizes whether each method is applicable in the static and modal analysis or not.

	Guyan reduction method	Symmetry	Geometry simplification	Multibody system
Static analysis	+	+++	++	+
Modal analysis	+++	++	++	++

Table 1. Application of simplification methods in static and modal analysis

The most common approach in daily practice is to just remove unnecessary grooves and fillets on a CAD model - Geometry simplification method. Also if possible, it is recommended to use an advantage of symmetry. Guyan reduction method is used in commercial FEA softwares including MSC-NASTRAN and ANSYS. Creation of multibody system highly depends on a particular study case.

All methods demand more or less of time for the preparation. An engineer has to decide, firstly, if the simplification method is applicable for a particular case and secondly, if a process of the model simplification does not consume more time than the full model analysis itself.

Finally, mechanical simulations should be followed by practical measurements in order to confirm reliability of both, measurements and simulations. This is especially true in the case when the model is simplified using any of the presented simplification methods.

3 Practical part

The main purpose of the practical part is to present several case studies which can show the reliability of model simplification methods presented in the theoretical part. The first study case is made as a multibody system. The second study case deals with Guyan static reduction method. In the third study case an example of a geometrical simplification is presented. In the fourth study case a cyclic symmetry is used in order to simplify the model.

3.1 Disks

Illustration in Figure 6 represents two disks connected with two shafts. One end of the left shaft is fixed to the wall. The material properties of the system are: Shear modulus $G = 7.69e^{10}\ Pa$ and density $\rho = 7850\ kg \cdot m^{-3}$, the geometrical parameters of the system are: $d_1 = 16\ mm,\ d_2 = 16\ mm,\ L_1 = 250\ mm,\ L_2 = 250\ mm,\ D_1 = 150\ mm,\ D_2 = 150\ mm,\ T_1 = 30\ mm$ and $T_2 = 30\ mm$. The main task is to study the system's behavior, particularly torsional vibrations of two disks – their natural frequencies.

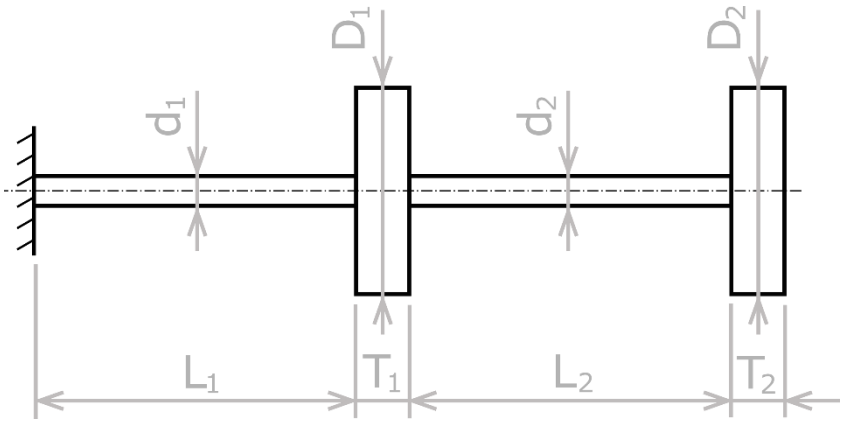

Figure 6. Model of the disks with dimensions

3.1.1 Full model analysis in ANSYS

In Figure 7, there is a 3D model created in ANSYS Workbench 18.0 according to the parameters above. The model is made as one flexible body. The model consists of 12 526 elements and 58 826 nodes. One end of the left shaft is fixed as shown in Figure 7. After performing the modal analysis, several modes are obtained (Table 2). The main interest is only in two torsional modes. In this case,

torsional modes are 3 and 6 with natural frequencies 40.192 Hz and 105 Hz respectively (torsional modes can be recognized from total deformation animations in ANSYS).

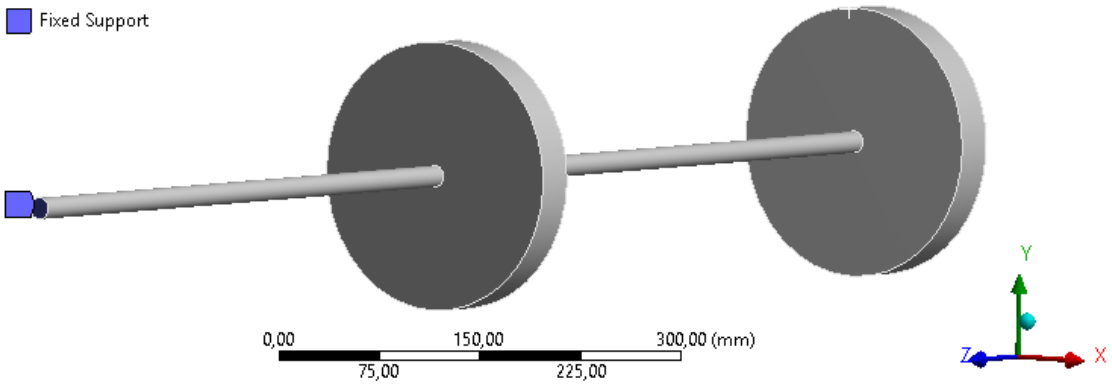

Figure 7. Full model – fixed support

Mode	**1**	**2**	**3**	**4**	**5**	**6**	**7**
Frequency [Hz]	8.0638	8.0643	40.192	53.311	53.319	105	186.170

Table 2. Modes with corresponding frequencies

3.1.2 Simplified multibody model

Figure 8 illustrates a simplified multibody model consisting of two inertias and two torsional springs. Inertias of springs are neglected. The system has the following parameters: torsional stiffness of the 1st spring k_{T_1}, torsional stiffness of the 2nd spring k_{T_2}, the 1st moment of inertia I_1 and the 2nd moment of inertia I_2. The system has 2 DOFs – rotations about x-axis.

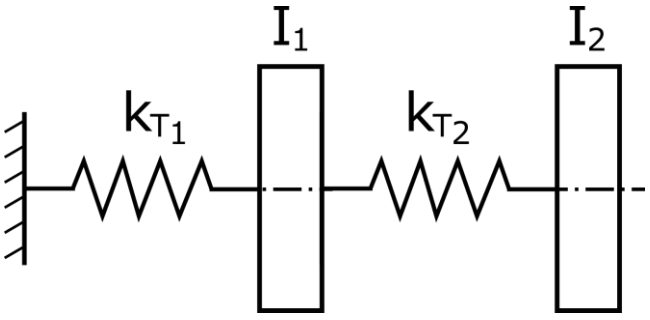

Figure 8. Simplified model

Pre-calculations

Firstly, simplified multibody model parameters are obtained from the dimensions of the full model. Beginning with masses of the disks

$$m_1 = \rho \cdot \pi \left(\frac{D_1}{2}\right)^2 \cdot T_1 = 7850 \cdot \pi \left(\frac{0.15}{2}\right)^2 \cdot 0.03 = 4.16\ kg \tag{16}$$

$$m_2 = \rho \cdot \pi \left(\frac{D_2}{2}\right)^2 \cdot T_2 = 7850 \cdot \pi \left(\frac{0.15}{2}\right)^2 \cdot 0.03 = 4.16\ kg \tag{17}$$

moments of inertia of the disks can be calculated as

$$I_1 = \frac{1}{2} m_1 \left(\frac{D_1}{2}\right)^2 = \frac{1}{2} \cdot 4.16 \cdot \left(\frac{0.15}{2}\right)^2 = 0.0117\ kg \cdot m^2 \tag{18}$$

$$I_2 = \frac{1}{2} m_2 \left(\frac{D_2}{2}\right)^2 = \frac{1}{2} \cdot 4.16 \cdot \left(\frac{0.15}{2}\right)^2 = 0.0117\ kg \cdot m^2 \tag{19}$$

Polar moments of inertia of the shafts are

$$J_{P_1} = \pi \frac{d_1^4}{32} = \pi \frac{0.016^4}{32} = 6.434\mathrm{e}^{-9}\ mm^4 \tag{20}$$

$$J_{P_2} = \pi \frac{d_2^4}{32} = \pi \frac{0.016^4}{32} = 6.434\mathrm{e}^{-9}\ mm^4 \tag{21}$$

From which can be calculated torsional stiffness of the springs

$$k_{T_1} = \frac{G \cdot J_{P_1}}{L_1} = \frac{7.69e^{10} \cdot 6.434\mathrm{e}^{-9}}{0.25} = 1979.69\ \frac{N \cdot m}{rad} \tag{22}$$

$$k_{T_2} = \frac{G \cdot J_{P_2}}{L_2} = \frac{7.69e^{10} \cdot 6.434\mathrm{e}^{-9}}{0.25} = 1979.69\ \frac{N \cdot m}{rad} \tag{23}$$

Calculations

Equations of motion can be derived using Newton's force method. Figure 9 shows the free body diagram of the system.

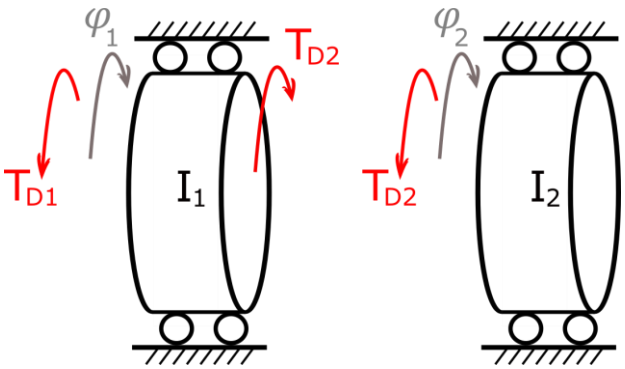

Figure 9. Free body diagram

Equations of motion are

$$I_1 \cdot \ddot{\varphi}_1 = \sum T_{1i} = -T_{D1} + T_{D2} \tag{24}$$

$$I_2 \cdot \ddot{\varphi}_2 = \sum T_{2i} = -T_{D2} \tag{25}$$

Reaction torques are

$$T_{D1} = k_{T_1} \Delta l_1 = k_{T_1} \varphi_1 \tag{26}$$

$$T_{D2} = k_{T_2} \Delta l_2 = k_{T_2} (\varphi_2 - \varphi_1) \tag{27}$$

where Δl_1 and Δl_2 are angular displacements.

Introducing Eq. (26) and (27) into Eq. (24) and (25) produces

$$I_1 \cdot \ddot{\varphi}_1 + k_{T_1} \varphi_1 - k_{T_2} (\varphi_2 - \varphi_1) = 0 \tag{28}$$

$$I_2 \cdot \ddot{\varphi}_2 + k_{T_2} (\varphi_2 - \varphi_1) = 0 \tag{29}$$

and after reordering

$$I_1 \cdot \ddot{\varphi}_1 + \left(k_{T_1} + k_{T_2}\right) \varphi_1 - k_{T_2} \varphi_2 = 0 \tag{30}$$

$$I_2 \cdot \ddot{\varphi}_2 - k_{T_2} \varphi_1 + k_{T_2} \varphi_2 = 0 \tag{31}$$

Eq. (30) and Eq. (31) can be written as

$$\begin{bmatrix} I_1 & 0 \\ 0 & I_2 \end{bmatrix} \cdot \begin{Bmatrix} \ddot{\varphi}_1 \\ \ddot{\varphi}_2 \end{Bmatrix} + \begin{bmatrix} k_{T_1} + k_{T_2} & -k_{T_2} \\ -k_{T_2} & k_{T_2} \end{bmatrix} \cdot \begin{Bmatrix} \varphi_1 \\ \varphi_2 \end{Bmatrix} = \begin{Bmatrix} 0 \\ 0 \end{Bmatrix} \tag{32}$$

Assuming the solution as

$$\varphi_{1(t)} = C_1 \cdot \sin(\Omega_0 \cdot t + \varphi) \tag{33}$$

$$\varphi_{2(t)} = C_2 \cdot \sin(\Omega_0 \cdot t + \varphi) \tag{34}$$

and

$$\ddot{\varphi}_{1(t)} = -C_1 \cdot {\Omega_0}^2 \cdot \sin(\Omega_0 \cdot t + \varphi) \tag{35}$$

$$\ddot{\varphi}_{2(t)} = -C_2 \cdot {\Omega_0}^2 \cdot \sin(\Omega_0 \cdot t + \varphi) \tag{36}$$

where Ω_0 is a natural frequency and φ is an initial phase angle.

And substituting solution into Eq. (30) and Eq. (31) is obtained

$$(k_{11} - \lambda \cdot I_1) \cdot C_1 + k_{12} C_2 = 0 \tag{37}$$

$$k_{21} C_1 + (k_{22} - \lambda \cdot I_2) \cdot C_2 = 0 \tag{38}$$

which can be written as

$$(K - \lambda \cdot M) \cdot v = 0 \tag{39}$$

System of equations has a trivial solution. Searching for non-trivial solution $C_1 \neq 0$, $C_2 \neq 0$, determinant of the expression in brackets has to be equal to zero

$$\begin{gathered} |K - \lambda \cdot M| = \begin{vmatrix} k_{11} - \lambda \cdot I_1 & k_{12} \\ k_{21} & k_{22} - \lambda \cdot I_2 \end{vmatrix} = \\ = I_1 I_2 \lambda^2 - (k_{11} \cdot I_2 + k_{22} \cdot I_1) \cdot \lambda + k_{11} \cdot k_{22} - k_{21} \cdot k_{12} = 0 \end{gathered} \tag{40}$$

This is the quadratic equation with the eigenvalue λ as an unknown parameter. After inserting calculated values the quadratic equation results into

$$\lambda_1 = 64604.9\ s^{-2} \qquad \Omega_1 = \sqrt{\lambda_1} = 254.1749\ s^{-1} \qquad f_1 = \frac{\Omega_1}{2\pi} = 40.4532\ Hz \tag{41}$$

$$\lambda_2 = 442808.45\ s^{-2} \qquad \Omega_2 = \sqrt{\lambda_2} = 665.4385\ s^{-1} \qquad f_2 = \frac{\Omega_2}{2\pi} = 105.9078\ Hz \tag{42}$$

In order to get results and make changes quickly, all equations from this section were implemented in MATLAB code.

3.1.3 Results

Natural frequencies of simplified and full model and a relative error are written in Table 3. The relative error δ in percents is calculated using formula

$$\delta = \frac{f_S - f_F}{f_F} \cdot 100 \tag{43}$$

where f_F is a natural frequency of the full model and f_S is a natural frequency of the simplified model.

Observing natural frequencies, it can be seen that the natural frequency of the simplified model is higher than the frequency of the full model. A relative error for the first mode is 0.6 % and for the second mode is 0.9 % which is a very small error.

Natural frequencies [Hz]			
	Full	**Simplified**	**delta [%]**
Mode 1	40.1920	40.4532	0.6
Mode 2	105	105.9078	0.9

Table 3. Comparison of the natural frequencies

Considering several modifications of the model when the disks' diameters $D_1 = D_2 = D$ are equally changing and other dimensions remain the same (Figure 10), it can be observed how the ratio between the shaft diameter d and disk diameter D affects results. Figure 11 shows the relation between a relative error and a shaft/disk diameter ratio.

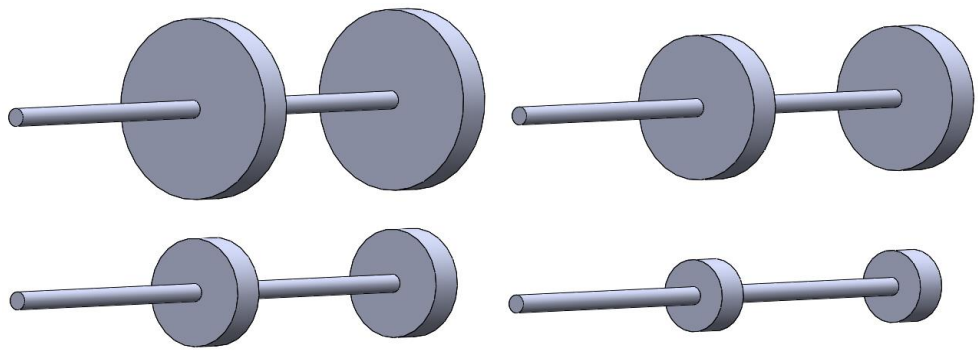

Figure 10. Changing of the shaft/disk diameter ratio

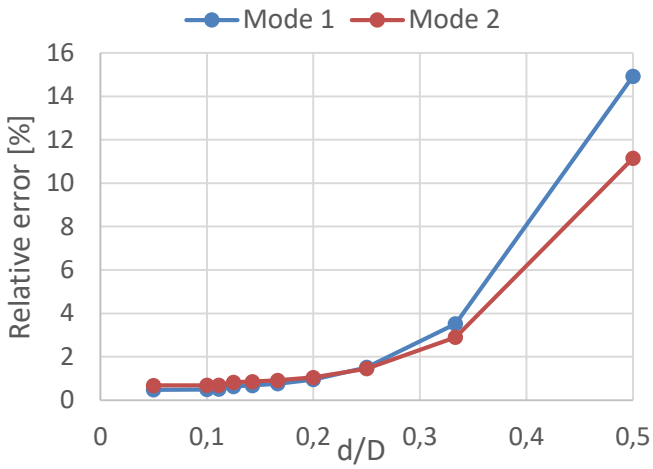

Figure 11. Relation between a relative error and a shaft/disk diameter ratio

3.1.4 Discussion

In this case, it can be concluded that the results obtained from the simplified model are accurate. Because of using different software for calculating the full and simplified model, the time for solving the analysis was not provided. Nevertheless, the solution time can be presented as the number of degrees of freedom entering the analysis. Comparing the full model with thousands of DOFs and the simplified model with only two DOFs, in can be concluded that the solution time was significantly reduced. However, the solution time does not include time for the model's preparation. In this case, creating and analyzing of the simplified model and analyzing of the full model were both quick procedures. Considering a more complex structure, a simplification process can take a lot of time (as mentioned in Chapter 2.5), therefore, an engineer has to consider which option is the best for the particular case, if to analyze the full model or to make the simplification.

The advantage of a simple model is that it is easy to perform a sensitivity analysis and study how sensitive the system is for certain parameter changes. In this case was examined how the changing of the model dimensions affects results. It has to be noted that the inertias of the shafts were neglected due to the big difference between the diameter of the disk and shaft. If both diameters are close to each other (d/D increases to 0.5 as shown in Figure 11), inertias of the shafts cannot be neglected.

3.2 Beam

A cantilever beam is shown in Figure 12. One end of the beam is fixed. The geometrical parameters of the beam are $L = 200\,mm$, $H = 20\,mm$ and $B = 20\,mm$. The material properties of the beam are Elastic modulus $E = 210000\,MPa$ and density $\rho = 7850\,kg \cdot m^{-3}$.

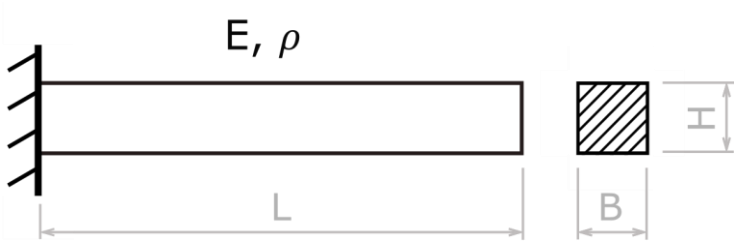

Figure 12. Cantilever beam

MATLAB code developed and provided by Dr. Jussi Sopanen is used to create the finite element model of the beam, and perform full model analysis, Guyan reduction method and simplified model analysis. [19]

The FE model of the beam in Figure 13 consists of 8 elements and 9 nodes. Each node has three DOFs: translation in x-axis, translation in y-axis, and rotation in x-y plane. The full model has 27 DOFs. The node no. 1 is fully constrained. The natural frequencies for the first three modes of the model are 41.5807 Hz, 249.3972 Hz, and 649.6355 Hz respectively. The mode shapes are shown in Figure 14.

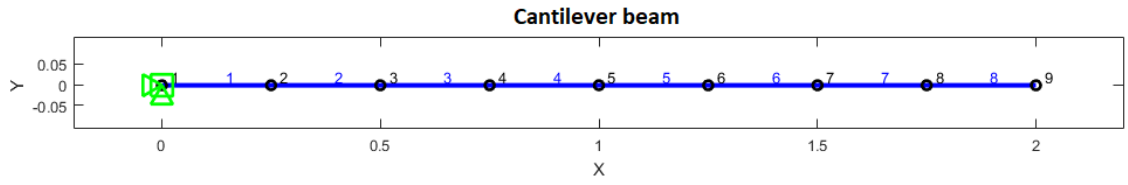

Figure 13. Finite element model of the cantilever beam

The reduced model is created using Guyan reduction method (the procedure is explained in Chapter 2.1.2) by selecting master nodes 4, 6 and 9. Each node has 3 DOFs, therefore the reduced model has 9 DOFs. The calculated natural frequencies of the reduced model are 41.5927 Hz, 250.3926 Hz and 656.6683 Hz.

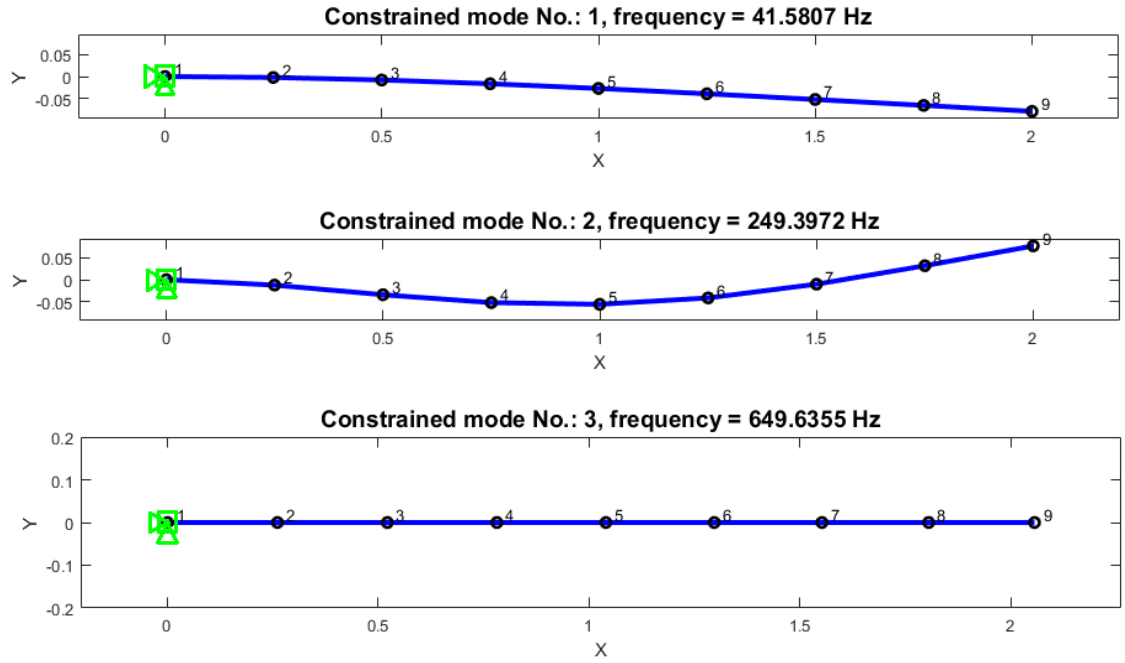

Figure 14. Mode shapes of the cantilever beam

Let us see how the natural frequencies change using different master nodes. Table 4 describes several variations of selected master nodes and corresponding natural frequencies of the first three modes.

Master nodes	2, 9	4, 8	5, 8	2, 5, 9	4, 6, 8	4, 6, 9	5, 6, 7	Full
Mode 1	41,647	41,601	41,591	41,612	**41,586**	41,593	41,632	**41,581**
Mode 2	273,202	253,639	253,013	251,351	250,640	**250,393**	258,325	**249,397**
Mode 3	670,090	661,628	657,596	664,355	**653,076**	656,668	659,522	**649,636**

Table 4. Selected master nodes and corresponding natural frequencies

3.2.1 Results

Using Guyan static reduction method it can be seen from Table 4 that the selected master nodes 4, 6, 8 give the closest values to the full system's 1st and 3rd natural frequencies, and master nodes 4, 6, 9 to the 2nd natural frequency. It can also be seen that the natural frequencies of the simplified models are all higher than the natural frequencies of the full model. This is because of Guyan reduction which makes the stiffness of the beam higher and mass of the beam lower.

Focusing on the 1st mode, it can be observed that all frequencies using different master nodes are very close to the full system frequency. It means that all nodes

(except the fixed node no. 1) participate in the 1st mode, so for the 1st mode frequency it does not matter that much which or how many nodes are set as master nodes. In the 2nd mode, the calculated frequencies using different master nodes, are also close to the full system's frequency. However, frequencies in the 3rd mode differ a lot using different master nodes. Generally, with higher modes the relative error is increasing.

3.2.2 Discussion

A simple example of the cantilever beam showed that using Guyan reduction method can significantly reduce the analysis time and provide accurate results, however selecting master degrees of freedom is crucial to obtain precise results. Therefore, the question: How to correctly select master degrees of freedom? has to be examined. The basic approach is to imagine a complex structure as a simple structure and then to observe how it acts. This may help to identify which parts of the complex structure contribute in certain modes.

From Table 4 it can be seen that choosing three master nodes yields to more precise results than choosing two master nodes, in other words, the more master nodes, the higher precision. However, comparing natural frequencies for all modes when master nodes are selected in the first case as 5, 8 and in the second case as 5, 6, 7, can be concluded that choosing more master nodes does not guarantee better results. This has to be also taken into account when selecting master degrees of freedom.

3.3 Simplification of the geometry

In this section, three examples are presented (Figure 15) to validate how the simplification of the geometry affects a static analysis. These examples were selected because of the variety of geometrical details and boundary conditions.

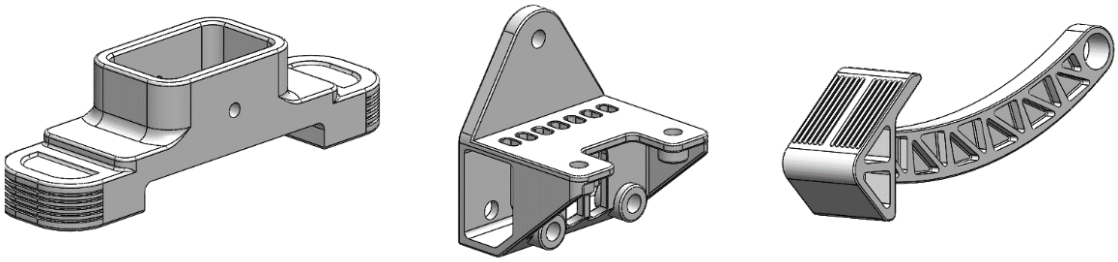

Figure 15. Case A, B and C (from the left to the right)

3.3.1 Models preparation

Figure 16 shows the boundary conditions BC applied on the full models (the same BC are applied on simplified models). Figure 17 presents the models after simplification. The following paragraphs describe how the models are simplified and what boundary conditions are used.

Case A – All grooves on the left and right side of the model are eliminated. A small hole going through the walls is suppressed and all small radiuses are removed. Only bigger radiuses which are considered as critical places are kept (Figure 17). The bottom of the model is fixed and the force was applied in the vertical direction on the upper face (Figure 16).

Case B – In this case, only small radiuses are removed (Figure 17). Constraints are applied on the holes where the part will be mounted with bolts to the wall. The force is applied on the horizontal desk in the normal direction (Figure 16).

Case C – Straight stripes on the pedal are removed and all small radiuses are eliminated (Figure 17). The hole is fully constraint and the force is applied on the stripes in the normal direction to their faces (Figure 16).

For both models - full and simplified - such a mesh was generated which corresponds to the model's shape and geometrical details. This guarantees obtaining precise results from the static analysis.

After an execution of a finite element analysis, the results between the original and the simplified model are compared, namely equivalent stress, total deformation and solution time.

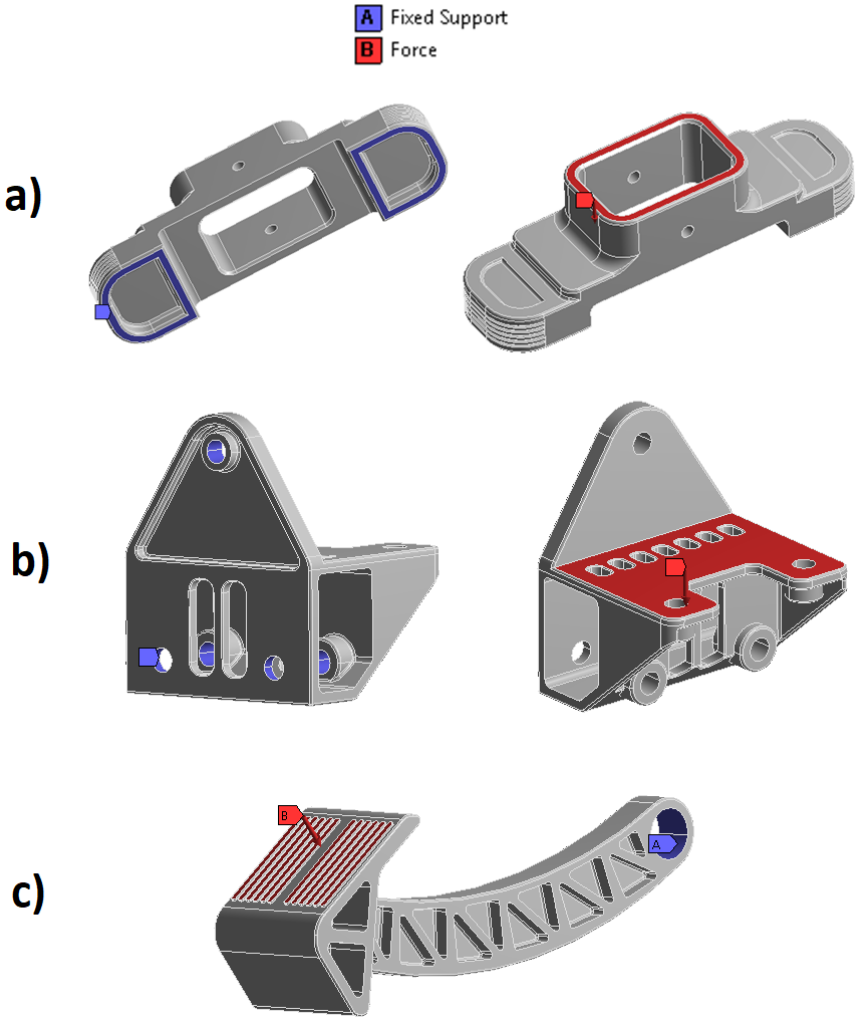

Figure 16. Boundary conditions – a) Case A, b) Case B, and c) Case C

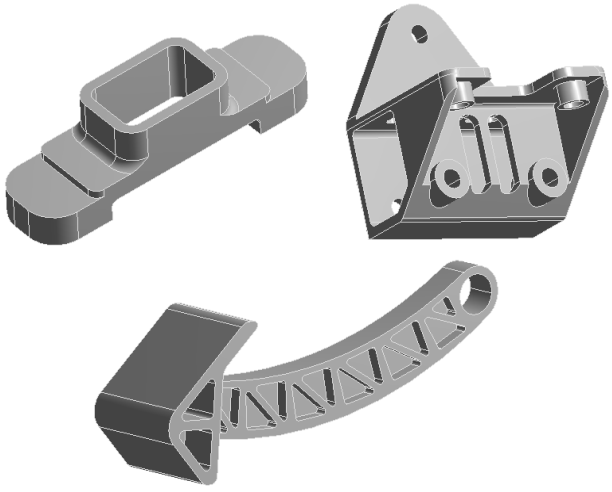

Figure 17. Simplified models

3.3.2 Results

Figures 18, 19 and 20 represent the results from the static analysis of the finite element models of the three studied parts before and after removing details. The results are summarized in Tables 5, 6 and 7. The left side of Figures 18, 19 and 20 shows the equivalent stress and the total displacement of the full model. The right side of Figure 18, 19 and 20 shows the equivalent stress and the total displacement of the simplified model.

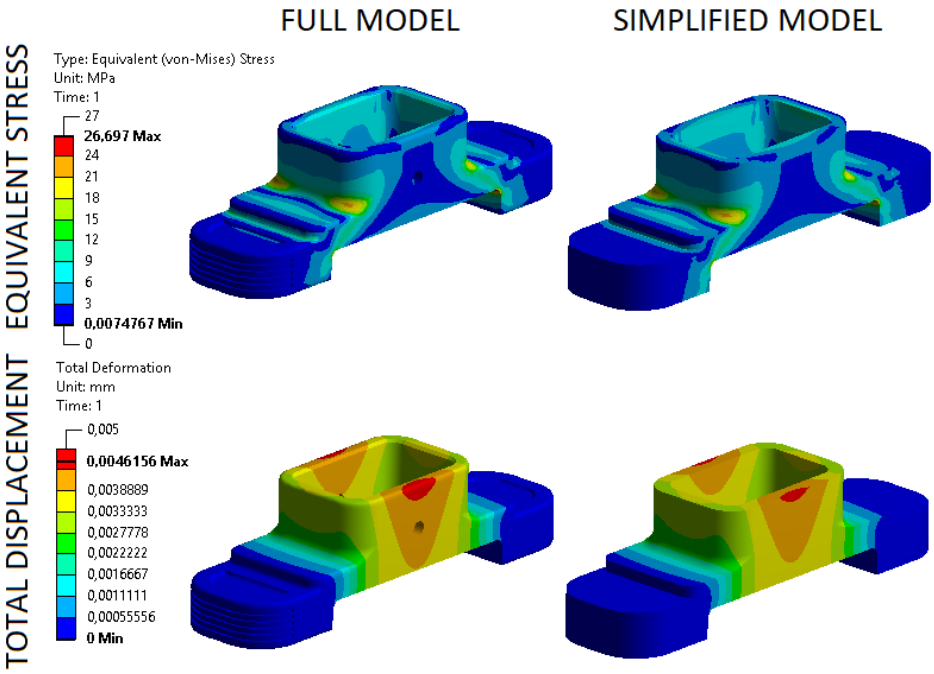

Figure 18. Stress and deformation results for the full and simplified model – Case A

CASE A	Full model	Simplified model	Percentage [%]
Max Stress [MPa]	26.697	25.698	3.74
Max Displacement [mm]	$4.62 \cdot 10^{-3}$	$4.57 \cdot 10^{-3}$	0.89
Solution time [sec]	28	18	35.71

Table 5. Comparison of stress and deformation results – Case A

For Case A, the computation time saved by simplification of the model is 36%. The equivalent stress error is 3.74% and the error related to the displacement is 0.89%.

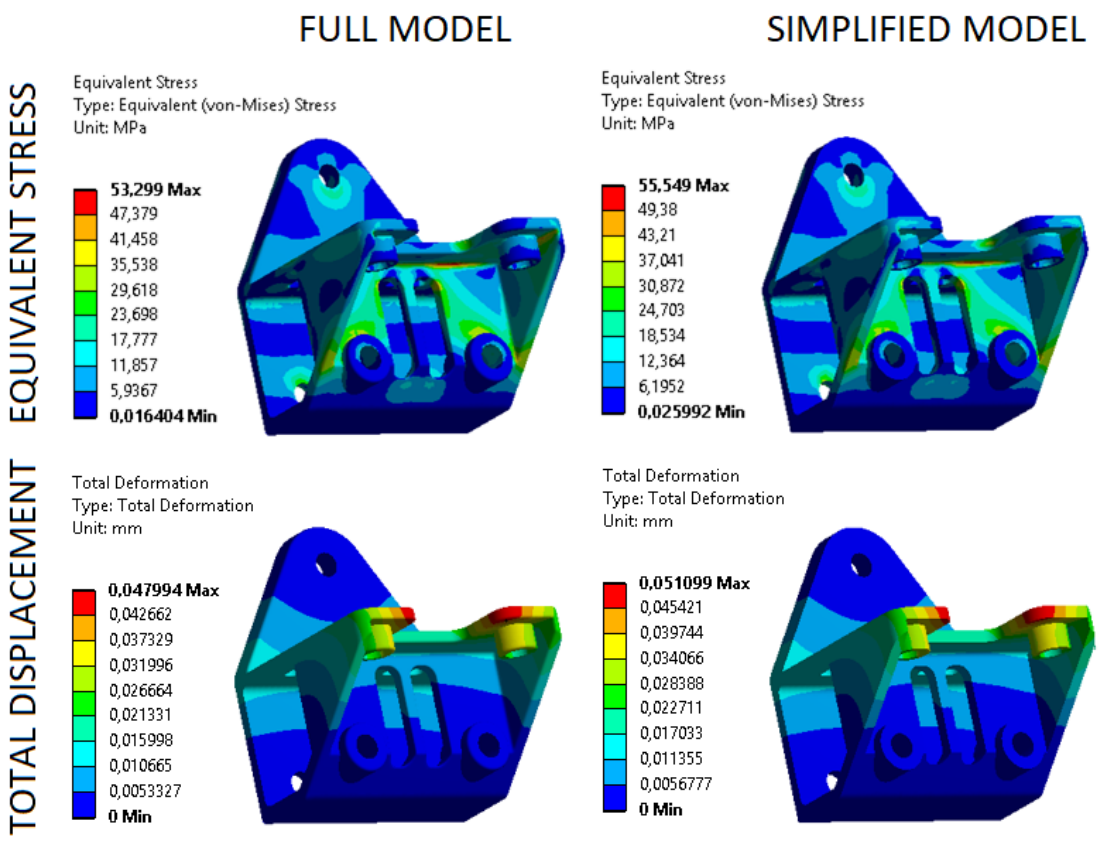

Figure 19. Stress and deformation results for the full and simplified model - Case B

CASE B	Full model	Simplified model	Percentage [%]
Max Stress [MPa]	53.299	55.549	4.22
Max Displacement [mm]	$4.8 \cdot 10^{-2}$	$5.11 \cdot 10^{-2}$	6.47
Solution time [sec]	38	29	23.68

Table 6 – Comparison of stress and deformation results – Case B

For Case B, the saved computation time is 24%, the equivalent stress is 4.22%, whereas the displacement error reaches the value 6.47%.

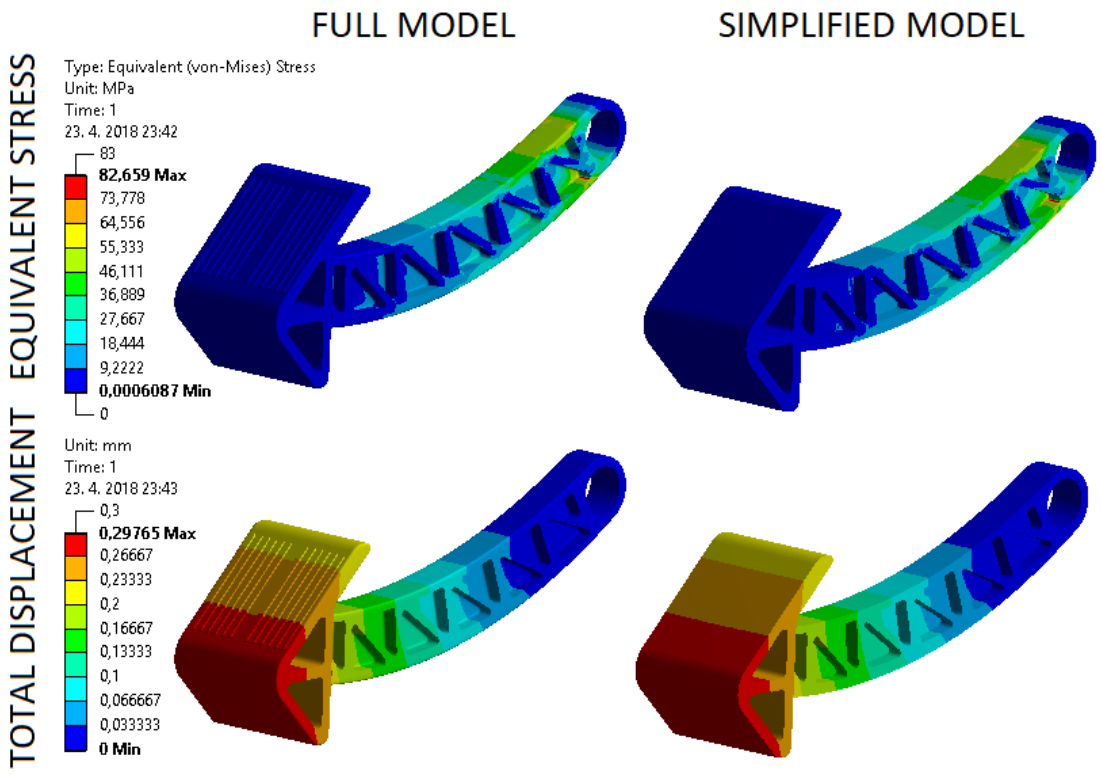

Figure 20. Stress and deformation results for the full and simplified model – Case C

CASE C	Full model	Simplified model	Percentage [%]
Max Stress [MPa]	82.659	82.814	0.19
Max Displacement [mm]	$2.98 \cdot 10^{-1}$	$2.99 \cdot 10^{-1}$	0.61
Solution time [sec]	30	19	36.67

Table 7. Comparison of stress and deformation results – Case C

For Case C, the saved computation time is 37%. The equivalent stress error is 0.19% and the displacement error is 0.61%.

Comparing the results of all three cases, it can be seen that for Case C, the simplification brought the highest saved computation time with a minimum error. It can be concluded that removing details on Case C did not affect the results of static analysis. Acceptance of errors of Case A and B has to be decided according to the model's purpose and function. Another noticeable point is that the simplification of the model causes increasing or decreasing of equivalent stress and the total deformation in a particular case.

3.3.3 Discussion

The whole process of simplification of the models was made manually using a 3D modelling software. Details such as small fillets, holes and grooves were considered to be removed from the full model, whereas several fillets and features were kept because they could significantly affect analysis results. This can be seen on Case A, where the maximum equivalent stress was found on one of the bigger fillets. In Case B, only small radiuses were removed. This caused around 4% stress error. Case C shows that changes on the geometry (e.g. removing stripes) made far from the critical place, do not affect the analysis results.

Manual removing of the details can take a long time, therefore it is convenient to use an algorithm as mentioned in Chapter 2.3, which makes the process automatic. However, it still has to be considered if the simplification and analysis of the model does not consume more time than a direct analysis of the full model.

3.4 Impeller

In this section a simplification using a cyclic symmetry is presented on an example of impeller (Figure 21). Firstly, the static analysis is performed on a full model and on one segment from the impeller. Secondly, the modal analysis is performed on the full model and on the segment. Analyses are made in ANSYS Workbench 18.0, the process of applying the cyclic symmetry in ANSYS is explained in the following section.

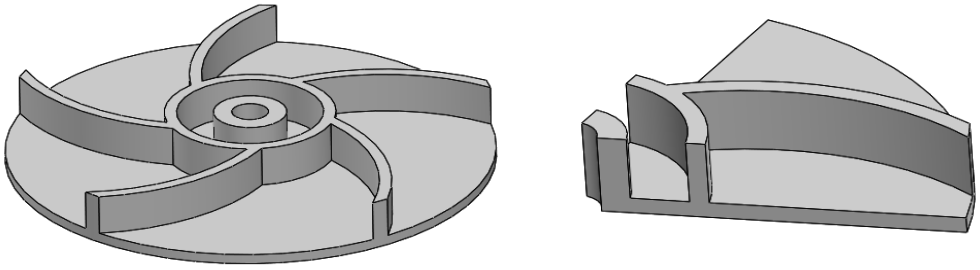

Figure 21. Models of the full impeller and its one segment

3.4.1 Modal cyclic symmetry in ANSYS

A modal cyclic symmetry analysis in ANSYS is carried out by creating constraint equations connecting the nodes on the low and high edge of the Basic and Duplicate sector (Figure 22). The edge with a lower angle in the cylindrical coordinate system is called the low edge and the one having the higher angle is called the high edge. In order to get the most precise results, it is recommended to create a Basic sector with an identical low and high edge. Then, a generated mesh has the corresponding nodes on each edge. During the solution stage, the program generates a duplicate sector of elements with the same geometric location as the basic sector, which is needed for displaying cyclic symmetry results.

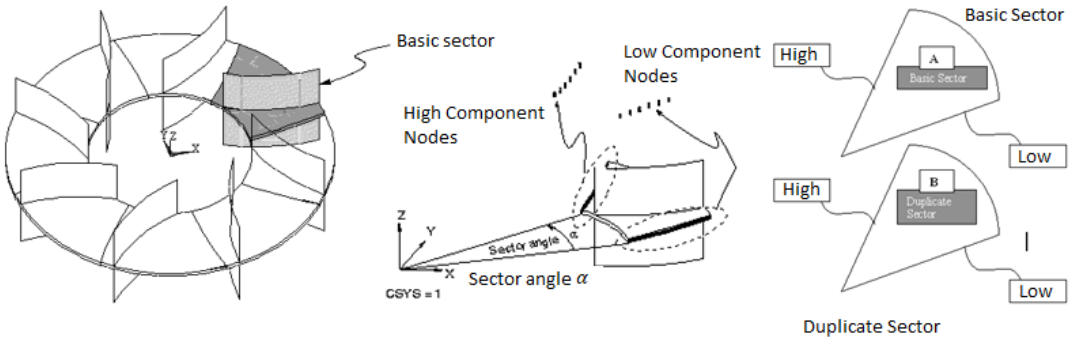

Figure 22. Basic and Duplicate sector [20]

Other key elements in a modal cyclic symmetry analysis are a nodal diameter and a harmonic index. Assuming a simple disc vibrating in a certain mode and observing its mode shapes, it can be seen lines of zero displacement which cross the entire disk. This line is called nodal diameter (Figure 23). The harmonic index is an integer that determines the variation in the value of a single DOF at points spaced at a circumferential angle equal to the sector angle (2π/n). The harmonic index range is from 0 to n/2 (n is even number) or to (n-1)/2 (n is odd number).

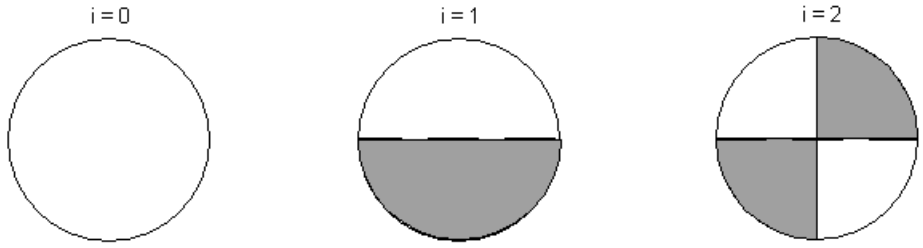

Figure 23. Examples of nodal diameters (i) [20]

The nodal diameter is the same as the harmonic index in only some cases. The relationship between the harmonic index k and the nodal diameter d for a model consisting of n sectors is:

$$d = m \cdot n \pm k, \quad m = 0, 1, 2 \ldots$$

Finally, the constraint equations for edge-component nodes are

$$\begin{Bmatrix} U^A_{High} \\ U^B_{High} \end{Bmatrix} = \begin{bmatrix} cosk\alpha & sink\alpha \\ sink\alpha & cosk\alpha \end{bmatrix} \begin{Bmatrix} U^A_{Low} \\ U^B_{Low} \end{Bmatrix}$$

where k is harmonic index, α is sector angle and U is a vector of displacement and rotational degrees of freedom. The equation is a function of harmonic index, and generates different sets of constraint equations for each harmonic index. [20]

3.4.2 Full model

A CAD model of the impeller was created in Solidworks. A base of the impeller is formed from a disk with a hole in the middle. The impeller has five blades connected with the ring, which are equally placed 72° from each other about the central axis. A generated mesh is made from tetrahedrons, the mesh contains 106 233 nodes and the number of elements is 60 855. Boundary conditions for a static analysis are displayed in Figure 24. A hole in the middle of the impeller is fully constrained. A rotational velocity 942 rad/s (9 000 RPM) is about z-axis of Global Coordinate System, which is located to the Centre of Gravity of the impeller. The results to be observed in the static analysis are equivalent stress and total deformation.

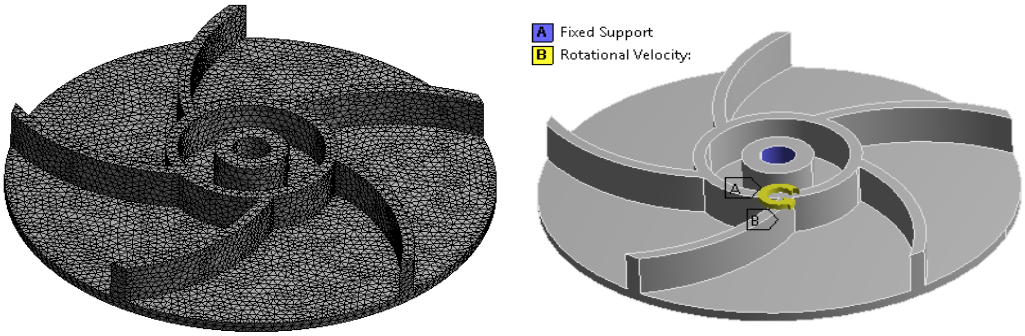

Figure 24. Full model - mesh (left) and boundary conditions (right)

As a boundary condition for the modal analysis the fixed support of the hole is chosen. The results to be observed in the modal analysis are natural frequencies and mode shapes. The main focus is on the first 6 modes.

3.4.3 One segment

The impeller contains a circular pattern of 5 sections. One section can be extracted to perform the modal analysis. A cut section, displayed in Figure 25, contains one blade, the angle between two cutting planes is 360/5=72°. Before creating a mesh, a new cylindrical coordinate system was created with x-axis in the radial direction, y-axis presenting the angle coordinate and z-axis in the axial direction. As explained in Chapter 3.4.1, a cyclic symmetry feature with its low and high boundary conditions has to be set up. A low boundary condition was selected on the right face and a high boundary condition was selected on the left face of the section according to the growing angle coordinate (Figure 25).

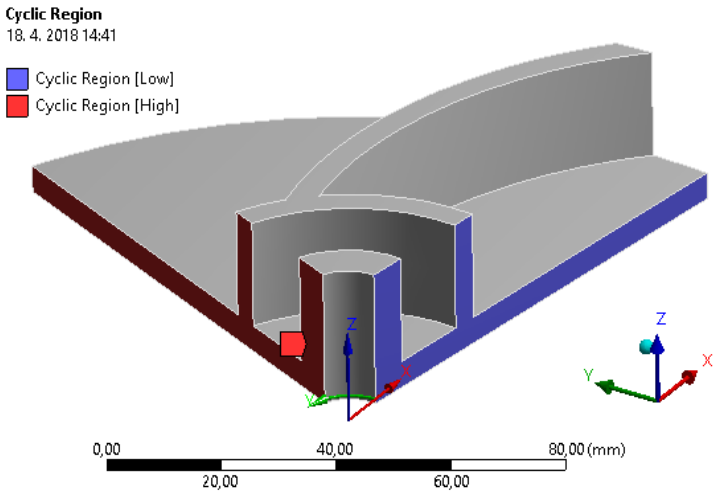

Fig. 25 – High and low edges

A mesh was created from tetrahedrons, the number of nodes in the mesh is 22 562 and the number of elements is 12 621 which is approximately 5 times less than in the full model (Figure 26).

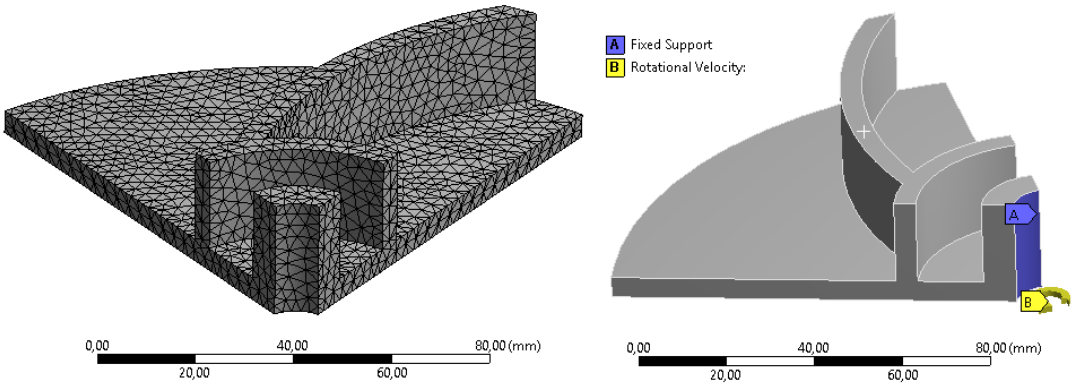

Figure 26. One segment - mesh (left) and boundary conditions (right)

Similarly, as in the full model, the boundary conditions for the static analysis applied on one section are fixed support for the inner surface of the hole and a rotational velocity 942 rad/s acting along z-axis of the cylindrical coordinate system (Figure 26). The results to be observed in the static analysis are equivalent stress and total deformation. A boundary condition in the modal analysis is a fixed support applied on the inner surface of the hole. The results to be observed are natural frequencies and mode shapes. The main interest is on the first 6 modes. In our case, a full model has 5 repeating segments, therefore the range of the harmonic indices is from 0 to (5-1)/2 = 2. Together it is 3 harmonic indices. However, setting up 6 modes in ANSYS analysis settings using a cyclic symmetry would result into a number of modes which is equal to a number of searched modes times a number of harmonic indices, in our case, it is 6x3=18 modes. In order to obtain just 6 modes from the analysis, a needed number of searched modes is 2.

3.4.4 Results – static analysis

Figure 27 shows the results from the static analysis – the equivalent stress and total deformation of the full model (on the left) and of one segment from the impeller (on the right). Even though just one segment of the impeller was analysed, ANSYS displays the whole model by multiplying the results of one segment.

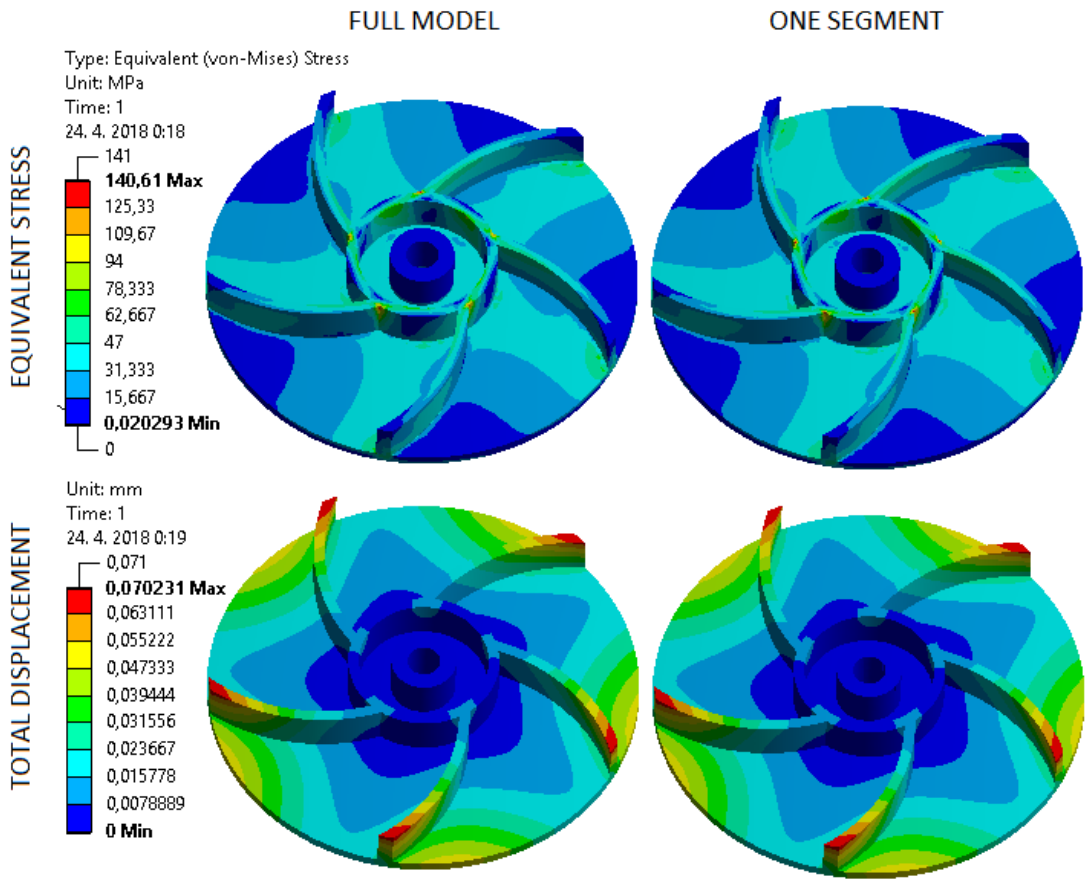

Figure 27. Stress and deformation results for the full model and one segment

The values of the maximum equivalent stress and the total deformation are written in Table 8. The equivalent stress error is 0.88% and the error related to the displacement is 0.1%. The solution time saved using a cyclic symmetry is 50%.

	Full model	**One section**	**Percentage [%]**
Max Stress [MPa]	140.61	139.37	0.88
Max Displacement [mm]	$7.02 \cdot 10^{-2}$	$7.02 \cdot 10^{-2}$	0.10
Solution time [sec]	22	11	50.00

Table 8. Comparison of stress and deformation results

3.4.5 Results – modal analysis

Beginning with the modal analysis of one segment, ANSYS provides results in a form of harmonic indices and its corresponding frequencies as shown in Table 9.

Mode	Harmonic index	Frequency [Hz]
1	0	1198.9
2	0	1235.9
1	1	647.41
2	1	647.41
1	2	1009.9
2	2	1009.9

Table 9. Results from the modal cyclic symmetry analysis

Agreed with the calculation before, there are 3 harmonic indices. The mode shapes corresponding to the natural frequencies are shown in Figure 28.

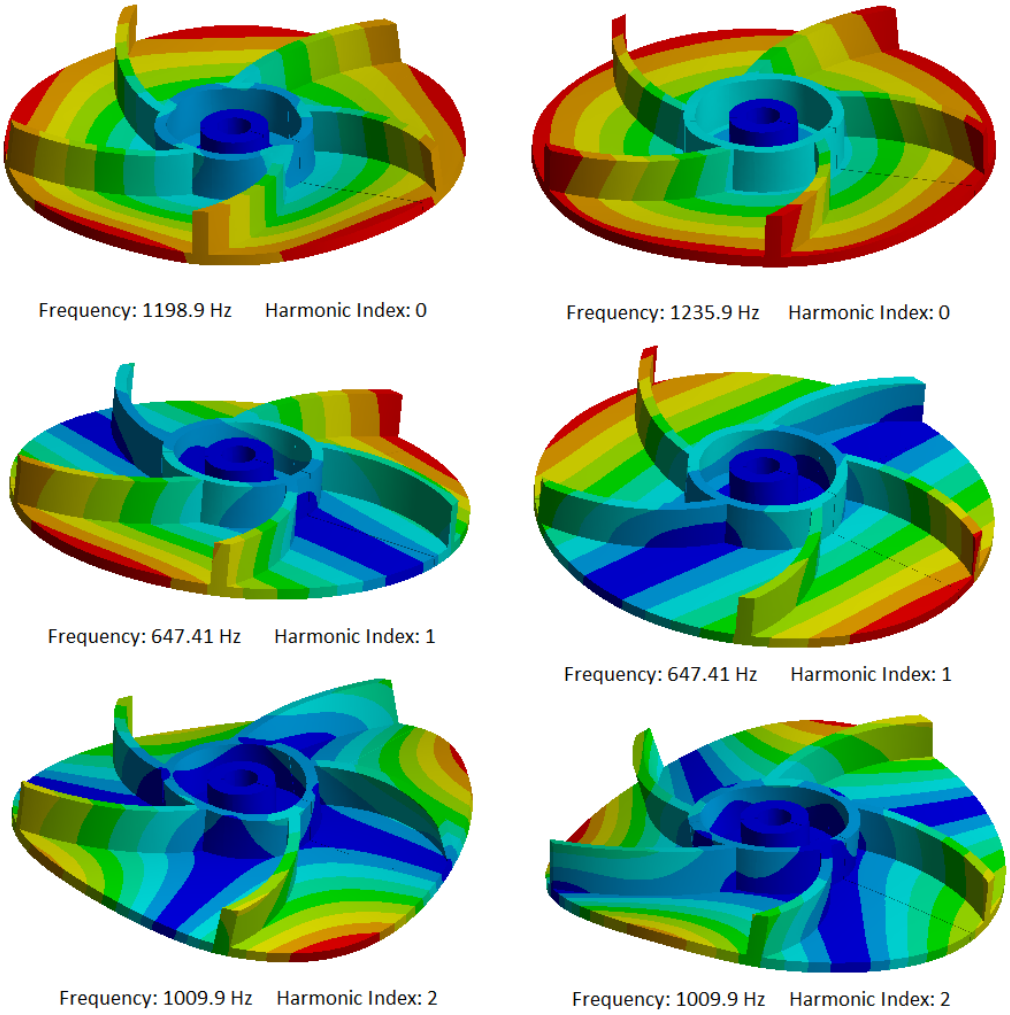

Figure 28. Mode shapes – harmonic index 0, 1 and 2 (from the top to the bottom)

The mode shapes of the harmonic index 0 represent the so called umbrella shape where the middle of the impeller is fixed and the rest is moving in the same direction up and down. The mode shapes of the harmonic index 1 represent a travelling wave passing through the circumference. The modes shapes are similar with 90° angle shift, their corresponding natural frequencies are the same. Mode shapes of the harmonic index 2 show two zero displacement planes perpendicular to each other. The mode shapes of the full model are not displayed because they are similar to the mode shapes of one segment.

Natural frequencies of one segment are sorted from the least to the highest frequency, and compared with natural frequencies of the full model in Table 10. A maximum relative error between natural frequencies is approximately 0.2%.

Mode	Full model frequency [Hz]	One segment frequency [Hz]
1	647.94	647.41
2	648.72	647.41
3	1009.8	1009.9
4	1009.8	1009.9
5	1199.2	1198.9
6	1236.2	1235.9

Table 10. Comparison of the natural frequencies of the full model and one segment

The solution time for analysing of the full model is 40 seconds and the analysis using cyclic symmetry takes 32 seconds, which makes a saving time 20%.

3.4.6 Discussion

The results from the static analysis state that the relative stress error is under one percent. The difference between the results of the full model and one section of the model can be caused due to a different mesh on each model. The advantage of the cyclic symmetry is that even a denser mesh can be generated on one segment in order to receive more precise results, and still it consumes less time for solving the analysis than analysing of the full model.

In this case, creating a cyclic symmetry saved 50% of the solution time in the static analysis. This work presented just one example, still it can be assumed that if a part would have had more cyclic segments, the saved solution time would significantly increase.

Setting up a cyclic symmetry in ANSYS is not difficult. However, it is necessary to calculate the number of harmonic indices before starting the analysis in order to set up the right number of modes as explained in Chapter 3.4.3.

In this work, the main interest was in the first 6 modes and the relative error between the natural frequencies turned out to be very small. Nevertheless, calculating more modes is needed to verify if cyclic symmetry in ANSYS provides acceptable results for higher frequencies.

4 Conclusion

The main goal of the thesis was to present four simplification methods for model reduction in mechanical analysis, and demonstrate their applicability on simple examples. For each example analysis of its full model and simplified model was performed. The results from both analyses were compared in order to verify the functionality of the methods.

In the first example, a multibody system was created based on the model of two disks connected with shafts. A relative error of natural frequencies for two modes did not reach 1%. It was also shown that if there is a small difference between the size of the disk diameter and the shaft diameter, the relative error significantly increases.

Another example of the cantilever beam demonstrated application of Guyan reduction method. Different master nodes were selected in order to observe how much selected nodes contribute on particular mode shapes. From the results it was visible that Guyan reduction method is beneficial in the modal analysis, however it highly depends which nodes are selected as master nodes.

Simplification of geometry was studied on three examples – Case A, B and C. The static analyses of models were performed. By removing unnecessary details from the models saving of the computation time up to 37% was achieved. Removing details had different impact on the results in each case. It was pointed out that several details cannot be removed, because they are a part of critical places where the maximum stress is.

In the last example, cyclic symmetry in ANSYS was applied on the model of the impeller. The solution time in the static analysis was reduced to 50% and in the modal analysis to 20%. It was shown that cyclic symmetry in ANSYS is easy to implement. The obtained results were precise enough reaching only the relative stress error 0.9% in the static analysis and the relative frequency error 0.2% in the modal analysis.

The thesis showed that applications of presented simplification methods were beneficial for reducing computational effort in mechanical analysis for the given

cases. In the future work, the main interest would lay on discovering more simplification methods followed with more complex examples.

Figures and tables

References

1. INMAN, D. J. *Engineering vibration*. Fourth edition. Boston: Pearson, 2014. ISBN 978-0132871693.

2. Chung, Y. T. *Model Reduction and Model Correlation Using MSC/NAS-TRAN.* MSC 1995 World Users' Conf. Proc., 1995.

3. QU, Zu-Qing. *Model order reduction techniques*. ISBN 18-523-3807-5, pp. 47-49.

4. Sopanen, J. *2017WK46_Lecture_10_FEM_Model_Reduction* [Lecture]. Lappeenranta, Lappeenranta University of Technology, 2017

5. Flanigan, C. C. *Model Reduction Using Guyan IRS and Dynamic Methods.* SPIE International Society for Optical Engineering, 1998, p. 174.

6. Barrett, P. *The Lost Art of Anti-Symmetry* [online]. https://caeai.com/blog/lost-art-anti-symmetry, 2017.

7. Madenci, E. and Guven, I. *The finite element method and applications in engineering using ansys*. Second Edition. New York, NY: Springer Science Business Media, 2014. ISBN 978-1489975492, pp. 20-21.

8. Foucault, G.; Cuillière, J.; FRANÇOIS, V.; LÉON J. and Maranzana, R. *Adaptation of CAD model topology for finite element analysis*. Computer-Aided Design, 2008, p. 178.

9. Rusu, C. *FEA basics – CAD model simplification for FEA analysis* [online]. 2013, http://feaforall.com/cad-model-simplification-for-fea-analysis/.

10. Yoon, Y. and Kim, B. C. *CAD model simplification using feature simplifications.* Journal of Advanced Mechanical Design, Systems, and Manufacturing. 2016.

11. Sheffer, A.; Blacker, T. D; and Bercovier, M. *Clustering: Automated detail suppresion using virtual topology*. Jerusalem, ASME, 1997.

12. Date, H.; Kanai, S.; Kisinami, T.; Nishigaki, I. and Dohi, T. *High-quality and property controlled finite element meshgeneration from triangular meshes using the multiresolutiontechnique*, Journal of Computing and Information Science in Engineering, 2005.

13. Lee, S. H. A. *CAD – CAE integration approach using feature-based multi resolution and multi-abstraction modelling techniques*, Computer-Aided Design, 2005.

14. Russ, B. H. *Development of a cad model simplification framework for finite element analysis* [online], University of Maryland, 2012, http://hdl.handle.net/1903/12447.

15. Bauchau, O.A. *Flexible multibody dynamics* [online]. Dordrecht: Springer, 2011, ISBN 978-940-0703-353.

16. Samin, J. and Fisette, P. *Multibody dynamics: computational methods and applications* [online]. New York: Springer, 2013, Computational methods in applied sciences (Springer (Firm)), v. 28. ISBN 978-94-007-5404-1.

17. Jia, J. *Essentials of applied dynamic analysis* [online]. Dordrecht: Springer, 2014, ISBN 978-364-2370-038.

18. 12” Heavy Duty Bench Grinder with Stand. In: *CANBUILT* [online]. http://www.canbuilt.com/catalogue_pdf/BG-1295HD.pdf. Accessed on 10 March 2018.

19. Sopanen, J. *2D_Beam_wk46* [Lecture]. Lappeenranta, Lappeenranta University of Technology, 2017

20. ANSYS, Inc. *ANSYS Release 18.0 Documentation*. 2016. Available in the electronic form in ANSYS 18.0.